[9] *Surface Texture*, American Standard ASA B46.1, 1962, The American Society of Mechanical Engineers, New York.

[10] Glenn, H. D. and Crowley, B. K., "Optical Technique for Monitoring High Energy Shocks in Steel Pipes Containing Ambient Atmospheric Air," Rept. UCRL-71007, 1968, Lawrence Radiation Lab., Livermore.

[11] Kapany, N. S., *Fiber Optics*, Academic Press, New York, 1967.

[12] Goettelman, R. C. and Crosby, J. K., "Optical Probe Techniques," *The Review of Scientific Instruments*, Vol. 35, No. 11, 1964, pp. 1546–1549.

[13] Crowley, B. K. and Glenn, H. D., "Numerical Simulation of a High Energy (Mach 120 to 40) Air Shock Experiment," presented at the Seventh International Shock Tube Symposium, Toronto, Canada, June 1969.

Supersonic Wake Flow Visualization

THOMAS J. MUELLER,* CHARLES R. HALL JR.,† AND WAYNE P. SULE‡
University of Notre Dame, Notre Dame, Ind.

Introduction

THERE has been great interest throughout the history of aerodynamics in making flow patterns visible. In addition to the qualitative picture of the flow hoped for, the possibility of obtaining quantitative flow measurements without introducing probes which invariably disturb the flow has provided the necessary incentive for development of these techniques. Optical methods of investigation which depend on density changes are especially suited to the visual study of supersonic flows. The interferometer, the schlieren, and the shadowgraph are commonly used optical methods of this type.

The use of smoke for flow visualization at low subsonic speeds is quite common and may be traced to L. Mach of Vienna in 1893.[1] Mach used an indraft low-speed wind tunnel (10 m/sec) with a piece of wire mesh to straighten the flow. The flow was observed and photographed by using silk threads, cigarette smoke, and glowing iron particles. The production of well-defined smoke streamlines (i.e., steady-state streaklines) at supersonic speeds was first accomplished by V. P. Goddard at the University of Notre Dame in 1959.[2] V. P. Goddard also developed a modified schlieren system that permits the simultaneous photographing of both the smoke and shock wave patterns. When nitrous oxide is used in place of smoke, the streamlines become visible along with the shock pattern in any ordinary schlieren system. The principal objectives of the investigation described herein were to extend and to improve supersonic flow visualization techniques for the study of laminar supersonic wake flows.

Experimental Apparatus and Technique

A schematic diagram of the small indraft planar supersonic smoke tunnel (PSST) utilized for these experiments is shown in Fig. 1. The PSST consists of inlet screens, contraction section, nozzle section including a plug which produces a wake, and a diffuser section. A total of seven inlet screens are located at the inlet to the contraction section in order to reduce the turbulence level of the flow. The contraction section has about a 100:1 contraction in area to the nozzle throat without the plug. With the plug in position, the contraction in area is about 200:1. The nozzle section consists of a contoured planar nozzle with a $\frac{1}{2}$-in. piece of lucite in the center of the nozzle block. The parallel outflow nozzle was designed for a Mach number of 1.40 and had a 2.5-in.[2] test section. A lucite wedge-shaped plug with a rounded leading edge was inserted into the nozzle to produce a wake. This configuration resembles a plug nozzle referred to as the expansion-deflection nozzle, or may be thought of as representing a strut, a flame holder, a scram-jet fuel injector, etc. The diffuser section connects the nozzle with a continuous operation vacuum pump that produces a pressure difference of 18 in. of mercury. A somewhat larger, though geometrically similar, PSST with a planar expansion-deflection nozzle test section was also used in this investigation. This larger nozzle section (i.e., about 4 in. × 5 in. in the working section downstream of the plug) contained an adjustable total and/or static pressure probe for conventional measurements. A complete description of this PSST is given in Ref. 3. Auxiliary equipment includes smoke generator and smoke rake, schlieren systems (to be described below), pressure taps, probes and manometers, high intensity lights, and a camera.

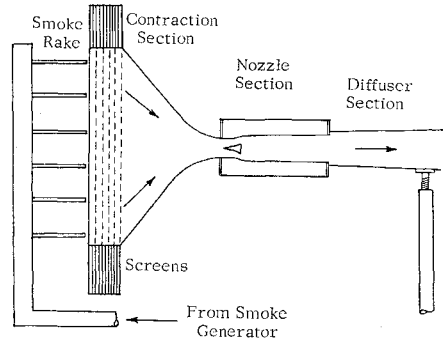

Fig. 1 Sketch of planar supersonic smoke tunnel.

A standard single-pass, parallel-light schlieren system was used. The standard schlieren system was converted to an opaque-stop system by replacing the slit source by a circular source and the knife edge by a small circular opaque-stop, i.e., a piece of glass with a $\frac{1}{16}$-in. diam spot. Proper adjustment of this system yields a schlieren picture where the undeflected light (i.e., no density gradient) hits the opaque stop producing a black background and deflected light misses the stop and shows up white. This black background is necessary for simultaneous schlieren and smoke photography. A single-frequency gas laser§ was also used as a light source in place of the 1000 w Bantam Super Spot in the opaque-stop schlieren system. Two double-convex lenses were used to diverge the laser beam for use in the schlieren system.

Smoke is generated by dripping kerosene on to electric strip heaters in each of the four legs of the generator. This smoke is forced to the smoke rake by a squirrel cage blower. By passing through a system of vertical pipes, the smoke is cooled to room temperature. Finally, the smoke passes through one or more of the horizontal tubes whose outlets are placed flush with the first screen at the PSST inlet. These tubes introduce the smoke into the PSST at any desired location.

Presented as Paper 69-346 at the AIAA 4th Aerodynamic Testing Conference, Cincinnati, Ohio, April 28–30, 1969; submitted April 23, 1969; revision received July 3, 1969. This research was jointly supported by the Department of Aerospace and Mechanical Engineering and NASA under Grant NsG(T)-65. The authors gratefully acknowledge the helpful comments of V. P. Goddard and A. A. Monkiewicz.

* Professor of Aerospace and Mechanical Engineering. Associate Fellow AIAA.

† NASA Fellow. Associate Member AIAA.

‡ Research Assistant. Associate Member AIAA.

§ Spectra-Physics Model 119, Helium-Neon Laser, wavelength 632.8 nanom, output power greater than 100 μw, uniphase, single frequency, beam divergence approximately 10 mrad.

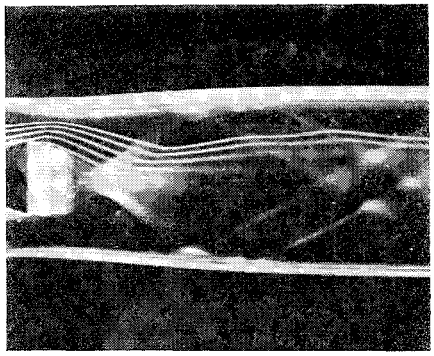

a) Direct smoke streamlines

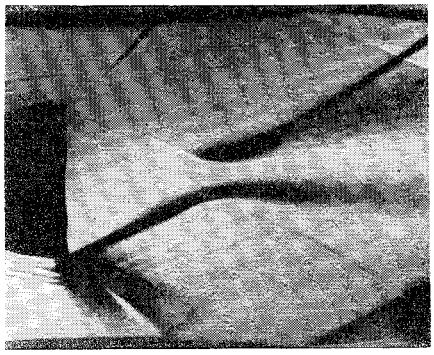

b) Nitrous oxide streamlines

Fig. 2 Photographs of wake flow with streamlines.

A bank of four quartz lights were placed about 1.5 in. from the nozzle section aligned with the lucite center. In addition, one or two high-spot flood lamps were usually aimed through the glass sidewall of the nozzle section at an angle of 45° to the flow. The schlieren photographs were taken with Royal Pan Film, 8 in. × 10 in., at an exposure of $\frac{1}{25}$ sec.

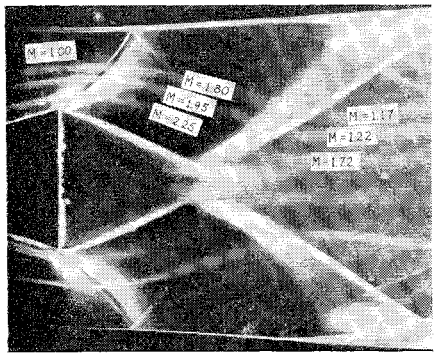

a) Bantam super spot light source

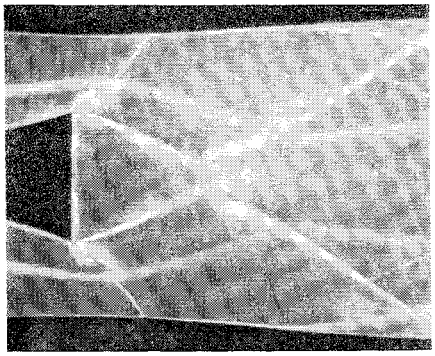

b) Gas laser light source

Fig. 3 Simultaneous smokeline and opaque-stop schlieren photographs of wake flow.

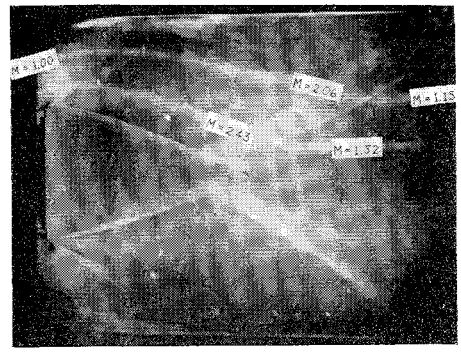

a) Simultaneous smokeline and opaque-stop schlieren

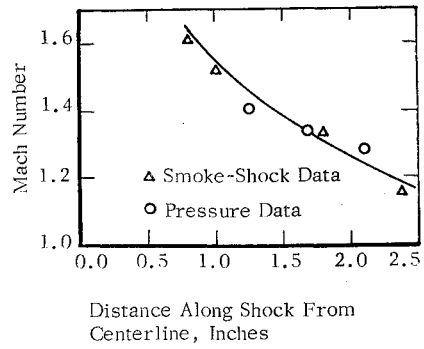

b) Correlation of visual and pressure data

Fig. 4 Correlation of smokeline shock data and pressure data for Mach number immediately downstream of recompression shock (E-D nozzle).

Direct smoke photography, i.e., not through the schlieren system, was also employed. A camera was mounted perpendicular to the flow and aimed at the region of interest through the glass sidewall. It was found that back lighting with the high-spot lamps produced the best results. Polaroid Type 57 film at about f-11 with an exposure of $\frac{1}{50}$ sec and Royal Pan film at about f-11 with a shutter speed of from $\frac{1}{10}$ to 1 sec gave good results.

Discussion of Visual Results from the Small PSST

An example of the results which can be obtained by direct photographing of smoke streamlines or simply smokelines is presented in Fig. 2a. The camera was aimed at the smokeline shock wave interaction downstream of the neck of the near wake; consequently, the view of the base region is not perpendicular to the flow in this photograph. The streamlines, i.e., steady-state streaklines, are very well defined upstream of the plug base and maintain this definition through the expansion about the separation corner and along the mixing region. The streamline next to the base region disappears in the vicinity of recompression where it seems to enter the trailing wake. The next streamline travels further downstream and then disappears. This phenomenon could be associated with the transition from laminar to turbulent flow in the trailing wake and/or the growth of the trailing wake. Figure 2a also shows that the upper two streamlines maintain their integrity through the entire flowfield indicating the change in direction which results from the shock waves that are present. The strong waves cause a dirt deposit to form on the glass sidewalls of the tunnel and can also be seen in this direct photograph. The location of the shock waves is somewhat different on the sidewalls than in the center of the test section as a result of the small but finite sidewall boundary layer.

By replacing the smoke generator with a bottle of nitrous oxide, streamlines may be observed on the standard schlieren system having a horizontal slit light source and knife edge, since nitrous oxide, unlike smoke, has a different index of

refraction than air. A schlieren photograph of the wake flow including nitrous oxide streamlines adjacent to the base region is shown in Fig. 2b. The streamlines appear clear upstream of the plug base, but become fainter after the expansion about the separation corner and along the mixing region. Further, these nitrous oxide streamlines become even fainter as the recompression oblique shock is approached, and are very difficult to see adjacent to the trailing wake. Furthermore, no significant density gradient perpendicular to the nozzle axis is indicated in the neck of the wake. The use of nitrous oxide or other suitable gases for streamline and/or streakline visualization appears to be very promising.

For steady flow, the smokeline is a streamline and can be used in conjunction with the model geometry and shock waves to determine Mach numbers in the flowfield. A simultaneous smokeline and opaque-stop schlieren photograph of the wake is presented in Fig. 3a. By measuring the local deflection and wave angles of the smoke streamlines passing through the recompression shock wave, the Mach numbers immediately ahead of and behind the recompression shock were determined and are shown in Fig. 3a. Dirt deposited on the glass sidewalls from a previous run is also visible in Fig. 3a. A simultaneous smokeline and opaque-stop schlieren photograph of the wake flow using the laser light source and "clean" glass sidewalls is presented in Fig. 3b.

Discussion of Visual and Probe Results from the Large E-D Nozzle PSST

A simultaneous smokeline and opaque-stop schlieren photograph of the planar expansion-deflection nozzle flowfield at its design operating conditions is presented in Fig. 4a The two smokelines are clearly visible in the top half of the photograph. Dirt on the glass sidewalls is also visible just upstream of the recompression shock waves. A comparison of the Mach numbers obtained from the streamline shock wave pattern of Fig. 4a and another photograph, and from total and static pressure measurements is shown in Fig. 4b. The correlation of Fig. 4b is for the Mach number immediately downstream of the recompression shock vs the distance measured along the recompression shock from the nozzle centerline. The agreement between the visual and pressure data is quite good.

Conclusions

Excellent direct photographs of the smoke streamlines were obtained. A composite streamline, shock and expansion wave patterns, was obtained by using nitrous oxide in place of smoke with an ordinary schlieren system and by using smoke with the opaque-stop schlieren system. From the simultaneous streamline-shock and expansion wave pattern, the Mach numbers adjacent to, but outside of, the viscous near wake and far wake were determined without introducing probes into the stream. For the E-D nozzle flow, a correlation of the visual and pressure data for the Mach number immediately downstream of the recompression shock vs distance along the shock from the nozzle centerline was quite good.

References

[1] Mach, L., "Uber die Sichtbarmachung von Luftstromlinien," *Zeitschrift fur Luftschiffahrt and Physik der Atmosphare*, Vol. 15, No. 6, 1896, pp. 129–139, plates I–III.

[2] Goddard, V. P., McLaughlin, J. A., and Brown, F. N. M., "Visual Supersonic Flow Patterns by Means of Smoke Lines," *Journal of the Aerospace Sciences*, Vol. 26, No. 11, Nov. 1959, pp. 761–762.

[3] Mueller, T. J., Hall, C. R., Jr., and Sule, W. P., "Experiments on the Two-Dimensional Expansion-Deflection Nozzle," AEDC-TR-67-279, Dec. 1967, Arnold Engineering Development Center, Air Force Systems Command, USAF.

Current Ratios in Coaxial Plasma Accelerators

R. P. Henry*
University of Ottawa, Ottawa, Canada
AND
D. S. Scott†
University of Toronto, Toronto, Canada

Since the generation of very large Hall currents may be important in certain types of coaxial plasma accelerators, plasma states yielding the most favorable conditions require investigation. Practical physical limitations usually restrict the current that may be carried by electrodes; however the Hall current, which is electrodeless and circulates within the body of the plasma, does not contribute as severely to electrode surface heating and resulting ablation problems.

Conditions yielding maximum Hall-to-applied currents may be calculated using a suitable generalized Ohm's law. In this Note, results based on the simple Cowling's law[1] are compared with a second approximation given by Demetriades and Argyropoulos.[2] This latter expression, developed by solving the Boltzmann equations according to Grad's "thirteen-moment" method, includes effects of electron-electron interactions and produces a more accurate determination of the inter-particle friction factors. Improved accuracy in the expression for scalar conductivity results.

When pressure and temperature gradients in the three-species plasma are neglected, both Ohm's laws assume the same form,

$$\mathbf{E}' = (1/\sigma)\mathbf{J} + \chi(\mathbf{J} \times \mathbf{B}) - \psi(\mathbf{J} \times \mathbf{B}) \times \mathbf{B} \qquad (1)$$

however, expressions for σ, χ, and ψ, the scalar conductivity, Hall coefficient, and ion slip coefficient differ. Now the factors in the square brackets of the following equations are no longer unity;

$$\frac{1}{\sigma} = \frac{m_e}{n_e e^2}\frac{1}{\tau_0}\left[1 - \frac{5}{2}\upsilon_0^2\tau_0\tau_e^*\right] \qquad (2)$$

$$\chi = \frac{1}{n_e e}\left[1 + \frac{5}{2}\upsilon_0^2\left(\frac{\tau_e^{*2}}{1 + \omega_e^2\tau_e^{*2}}\right)\right] \qquad (3)$$

$$\psi = \frac{2f^2}{n_e m_a}\tau_{ia}\left[1 + \frac{5}{4}\frac{m_a\tau_e^*}{f^2 m_e\tau_{ia}}\upsilon_0^2\left(\frac{\tau_e^{*2}}{1 + \omega_e^2\tau_e^{*2}}\right)\right] \qquad (4)$$

Collisions parameters υ_0 and τ_e^* are as defined in Ref. 2.

When use is made of Eq. (1), the expression for the ratio of Hall-to-electrode current is the same, except for a factor based on geometry, in the two common Hall current plasma accelerator configurations.[3] For a coaxial electrode geometry with axially applied magnetic field,

$$J_\theta/J_r = \chi\sigma B/(1 + \psi\sigma B^2) \qquad (5)$$

Introducing $\beta = \chi_0\sigma_0 B$ and $x = \chi_0^2\sigma_0/\psi_0$, where the subscript 0 refers to the Ohm's law coefficients in Cowling's expression, and

$$k_1 = \tfrac{5}{2}\upsilon_0^2\tau_0\tau_e^*, \quad k_2 = \tfrac{5}{2}\upsilon_0^2\tau_e^{*2}, \quad k_3 = \tfrac{5}{2}\upsilon_0^2\tau_e^{*3}/\tau_0 \qquad (6)$$

Presented as Paper 69-280 at the AIAA 7th Electric Propulsion Conference, Williamsburg, Va., March 3–5, 1969; submitted March 12, 1969; revision received July 25, 1969.

* Assistant Professor, Mechanical Engineering Department. Member AIAA.

† Associate Professor, Mechanical Engineering Department. Member AIAA.